



Cite this: *Chem. Commun.*, 2017, 53, 1723

Received 14th November 2016,  
Accepted 10th January 2017

DOI: 10.1039/c6cc09082f

www.rsc.org/chemcomm

## A bioorthogonal 'turn-on' fluorescent probe for tracking mitochondrial nitroxyl formation†

Kyoung Sunwoo,<sup>‡a</sup> Kondapa Naidu Bobba,<sup>‡b</sup> Ja-Yun Lim,<sup>‡c</sup> Taegun Park,<sup>c</sup> Arup Podder,<sup>b</sup> June Seok Heo,<sup>c</sup> Seung Gwan Lee,<sup>\*d</sup> Sankarprasad Bhuniya<sup>\*be</sup> and Jong Seung Kim<sup>\*a</sup>

**A bioreductant-resistant 'turn-on' chemodosimetric fluorescent probe Mito-1 has been developed for the detection of mitochondrial HNO in live cells. Mito-1 enables the detection of HNO as low as ~18 nM. It has the capability to detect both exogenous and endogenous mitochondrial HNO formations in cellular milieus by providing fluorescence images. Its two-photon imaging ability fosters its use as a non-invasive imaging tool for the detection of mitochondrial nitroxyl.**

Nitroxyl (NO<sup>-</sup>/HNO) is the one-electron reduced (and protonated) form of nitric oxide. This interconvertible pair plays a pivotal role in the nervous system.<sup>1</sup> HNO exhibits unique, distinct and often opposite pharmacological properties with its oxidized analogue NO.<sup>2</sup> For instance, NO donors reduce the  $\beta$ -adrenergic-stimulated contractility to minimize the use of  $\beta$ -agonists, whereas HNO is additive to the  $\beta$ -agonist dobutamine.<sup>3</sup> HNO inhibits the activity of various enzymes such as those containing thiols, including polymerase, the copper thiolate yeast transcription factor Ace1, aldehyde dehydrogenase and the zinc finger protein poly(ADP-ribose).<sup>4-6</sup> Additionally, its association with thiols alters the activity of the *N*-methyl-D-aspartate channel.<sup>7</sup> Moreover, HNO is capable of reacting with the thiol residue of various crucial enzymes in biological milieus. As an example, HNO reacts with glutathione (GSH) at a rate of  $2 \times 10^6 \text{ M}^{-1} \text{ s}^{-1}$  and depletes the function of GSH as a modulator in the cellular redox system.<sup>8,9</sup> While the conversion processes from nitrogen-based oxides and

superoxides have been reported as examples of HNO formation pathways, an endogenous formation of nitroxyl remains unclear because of its high reactivity with surrounding biomolecules (Fig. S1, ESI†).

Thus, it is crucial to sense HNO, as HNO is more cytotoxic than NO and can be potentially generated *in vivo*, and causes biological responses with some of the characteristics of NO and peroxynitrite. A class of fluorescent probes has been developed for sensing HNO, utilizing the reduction of Cu<sup>2+</sup> to Cu<sup>+</sup> or nitroxide to hydroxylamine.<sup>10,11</sup> Unfortunately, these probes suffer from interference by several highly abundant biological reductants, *e.g.*, GSH and ascorbate in the living system. Moreover, the detection limit for nitroxyl was not estimated.

To overcome the selectivity issue, recently Staudinger reaction chemistry-based bioorthogonal probes have been developed for sensing cellular HNO.<sup>12</sup> This chemodosimetric strategy<sup>13</sup> is free from interferences by biological reductants and has become a biologically viable strategy. By utilizing this chemistry, a couple of probes have been developed to detect HNO in lysosomes.<sup>14</sup> Indeed, the detection of HNO in mitochondria is quite important because the reaction of NO, associated with cancer metastasis,<sup>15</sup> with mitochondrial cytochrome *c* allows for the formation of nitroxyl (HNO). Moreover, HNO leads to inhibit mitochondrial respiration through the inhibition of complexes I and II, most probably *via* a modification of specific cysteine residues in the proteins.<sup>16</sup> Thus, our interest is to develop a metal free fluorogenic probe for HNO in mitochondria.<sup>17</sup> As presented in Scheme 1, the probe **Mito-1** was synthesized in two successive steps *via* an amide formation followed by esterification. The reaction procedures and spectroscopic analysis reports are available in the ESI† (Fig. S10–S17). We chose coumarin as a fluorophore because its high quantum yield and two-photon property may allow us to overcome optical interference from ubiquitous biological entities.<sup>18</sup>

To rationalize the sensitivity of **Mito-1** toward the bioanalyte HNO, we recorded UV-absorption and fluorescence changes of **Mito-1** in the presence of Angeli's salt (AS), a well-known HNO producing agent under physiological conditions. As shown in

<sup>a</sup> Department of Chemistry, Korea University, Seoul 136-701, Korea.  
E-mail: jongskim@korea.ac.kr

<sup>b</sup> Amrita Centre for Industrial Research & Innovation, Amrita School of Engineering, Amrita Vishwa Vidyapeetham, Ettimadai, Coimbatore 641112, India.  
E-mail: b\_sankarprasad@cb.amrita.edu

<sup>c</sup> Department of Integrated Biomedical and Life Sciences, College of Health Science, Korea University, Seoul 136-701, Korea

<sup>d</sup> Department of Health and Environmental Science, College of Health Science, Korea University, Seoul 136-701, Korea. E-mail: seungwan@korea.ac.kr

<sup>e</sup> Department of Chemical Engineering and Materials Science, Amrita School of Engineering, Amrita Vishwa Vidyapeetham, Ettimadai, Coimbatore 641112, India

† Electronic supplementary information (ESI) available: Synthesis procedure, NMR, MS, fluorescence, and cell imaging data. See DOI: 10.1039/c6cc09082f

‡ These authors contributed equally to this work.

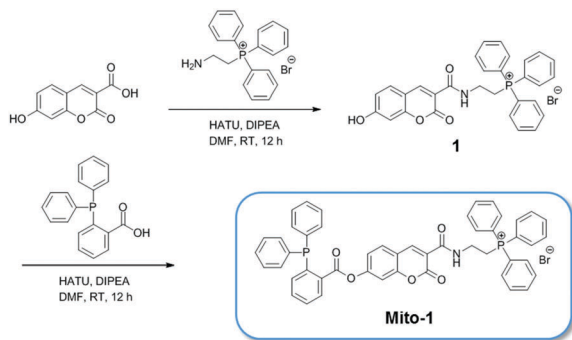
Scheme 1 Synthesis of **Mito-1**.

Fig. S2 (ESI<sup>†</sup>), the UV-absorption of **Mito-1** increased  $\sim 30$ -fold at 398 nm in the presence of AS (3 eq.). The fluorescence intensity at  $\lambda_{em}$  452 nm of **Mito-1** gradually enhanced with increasing concentrations of AS (0–100.0  $\mu$ M) and then reached saturation (Fig. 1A). It is demonstrated in Fig. 1A that the fluorescence intensity of **Mito-1** has a  $\sim 45$ -fold increase in the presence of HNO (AS) (100.0  $\mu$ M). Further applying a regression equation, the detection limit toward HNO was found to be 18.0 nM (Fig. S3, ESI<sup>†</sup>), which is considerably lower than reported probes (Fig. S4, ESI<sup>†</sup>).<sup>13,17</sup>

The temporal sensing of short-lived bio-analytes in biological milieus is a challenging task. Thus, we recorded time-dependent fluorescence intensity changes of **Mito-1** in the presence of HNO with the treatment of AS. The result in Fig. 1B indicates that in the presence of HNO (30.0  $\mu$ M) the fluorescence intensity of **Mito-1** reaches a maximum within 20 min. The rate constant of the reaction between **Mito-1** and nitroxyl was found to be

$1.0 \times 10^{-3} \text{ M}^{-1} \text{ s}^{-1}$  (Fig. S5, ESI<sup>†</sup>). This suggests that **Mito-1** may enable the detection of HNO in a cellular microenvironment within a short period of time.

Next, we checked whether **Mito-1** can react with HNO without any interference from other biologically relevant reactive species such as Cys, GSH, Hcy,  $\text{Na}_2\text{S}$ ,  $\text{H}_2\text{O}_2$ , NO,  $\text{NO}_3^-$ ,  $\text{NO}_2^-$ ,  $\text{O}_2^-$ ,  $\text{ROO}^\bullet$ , and  $\text{ClO}^-$ . Thus, we have monitored the changes of fluorescence intensity of **Mito-1** upon incubation with the aforementioned analytes at 25  $^\circ\text{C}$  for 20 min. As shown in Fig. 1C, the fluorescence intensity of **Mito-1** remains almost unaltered in the presence of other biologically relevant analytes, whereas **Mito-1** showed its fluorescence enhancement only in the presence of HNO (AS).

To validate the feasibility of the probe in a biological system where HNO is much less expressed compared to GSH, we tested the substrates under significantly different concentrations. Fig. S6 (ESI<sup>†</sup>) shows the result when 400 eq. of GSH and 6 eq. of HNO are treated. Although GSH shows a certain extent of reactivity with **Mito-1**, HNO reveals the outstanding fluorescence intensity even with its noticeably lower concentration. The exquisite sensitivity of **Mito-1** suggests that the probe is an excellent tool for sensing HNO in a cellular micro-compartment even in the presence of other short-lived chemical entities.

To clarify that the result is due to HNO instead of other byproducts of Angel's salt, we performed the reaction of AS and **Mito-1** in the presence of GSH, a scavenger of HNO. As the GSH concentration increased from 0 to 20  $\mu$ M, the fluorescence intensity decreased as expected, confirming that HNO is responsible for the increase in fluorescence intensity (Fig. S7, ESI<sup>†</sup>).<sup>12a</sup>

In addition, we analyzed the stability of **Mito-1** and its reactivity toward HNO in a variable pH range. The results in Fig. 1D indicate that **Mito-1** is quite stable within the physiological pH range (pH 4–8) and its reactivity toward HNO is optimized at pH 8, as the fluorescence intensity reached its maximum. As the mitochondrial matrix is slightly alkaline (pH  $\sim 8$ ),<sup>19</sup> we expect that **Mito-1** enables the detection of endogenous HNO in mitochondria.

Before proceeding to apply **Mito-1** for the sensing of exogenous/endogenous HNO in cellular milieus, we have evaluated its reaction mechanism with HNO as proposed in Scheme 2. Angel's salt (AS) treated **Mito-1** in acetonitrile was subjected to liquid chromatography-mass spectrometry (LC-MS) and HR-MS analyses. The LC-MS data in Fig. S8 (ESI<sup>†</sup>) indicated that two major components have presented in the chromatogram. The peaks at 322.1 and 494.2 match with the byproduct ( $M + 1$ ) and free fluorophore **1**, respectively. Also in the HR-MS data (Fig. S9, ESI<sup>†</sup>), a major peak appeared at 494.05, which corresponds to the fluorophore (**1**). This finding strongly approves our proposed intramolecular Staudinger reaction mechanism (Scheme 2).

The chemoselective 'turn-on' fluorescence changes of **Mito-1** toward HNO encourage us to utilize it for the detection of exogenous/endogenous HNO formation in mitochondria *via* its optical modulation. The cytotoxicity of **Mito-1** was assessed in HeLa cells using a SensoLyte<sup>®</sup> Cell Cytotoxicity Assay Kit, revealing no significant cytotoxicity at 10  $\mu$ M, thus confirming the excellent biocompatibility of the probe (Fig. S19, ESI<sup>†</sup>). Angel's salt-pretreated HeLa cells were incubated with variable

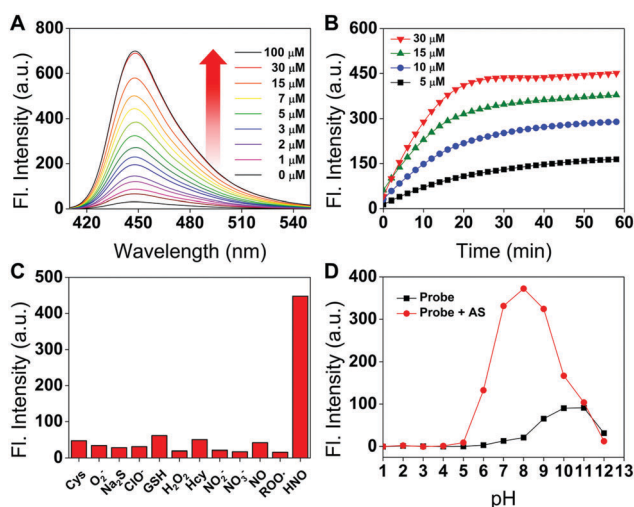
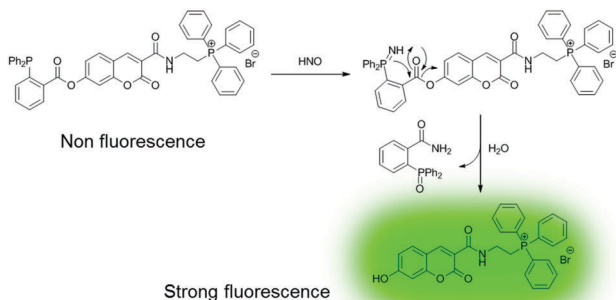
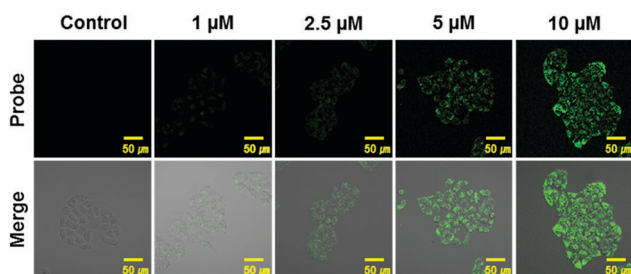


Fig. 1 Fluorescence response of probe **Mito-1**. (A) Fluorescence spectra of the probe (5.0  $\mu$ M) in pH 7.4 PBS buffer (0.5% DMSO) in the absence or presence of AS. The spectra were recorded after incubation of the probe with AS for 30 min. (B) Reaction–time profiles of the probe (5.0  $\mu$ M) in the presence of various concentrations of AS. The fluorescence intensities at 452 nm were continuously monitored at time intervals in pH 7.4 PBS buffer (0.5% DMSO). (C) The fluorescence responses of the probe (5.0  $\mu$ M) to various relevant species (30  $\mu$ M) in pH 7.4 PBS buffer. Emission at 452 nm. (D) The fluorescence intensity dependency of the probe (5.0  $\mu$ M) in the absence and presence of AS (30  $\mu$ M) on diverse pH values.

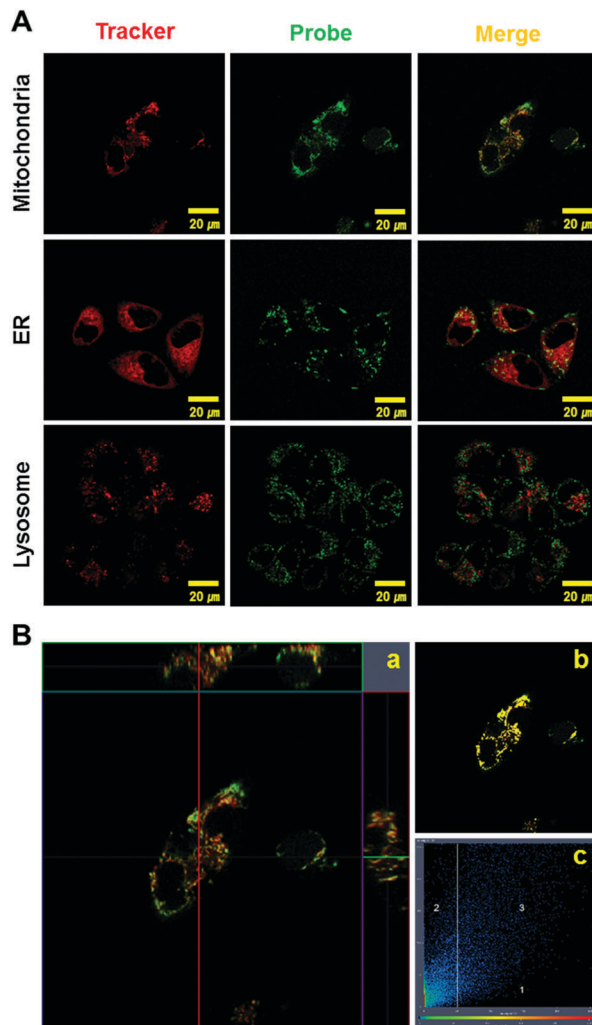
Scheme 2 Reaction mechanism between **Mito-1** and HNO.Fig. 2 Fluorescence images of exogenous HNO. Confocal microscopy images of the dose dependency of **Mito-1** fluorescence (magnification,  $\times 20$ ).  $\lambda_{\text{ex}}$  405 nm;  $\lambda_{\text{em}}$  470–500 nm.

concentrations of **Mito-1**. As shown in Fig. 2, the extent of cell-labeling increased in a dose-dependent manner.

As shown in Fig. 3, the exogenous nitroxyl in mitochondria was assessed by monitoring the fluorescence signal from **Mito-1**. We found that **Mito-1** was predominantly localized in mitochondria<sup>20</sup> compared with other organelles such as endoplasmic reticulum (ER) and lysosome (Lyso). Furthermore, the confocal Z-section images and co-localization scatterplots indicate that **Mito-1** was well co-localized with the Mito-tracker. These results suggest that **Mito-1** has the ability to track exogenous nitroxyl in mitochondria in living cells.

Next, we tracked the endogenous HNO formation in mitochondria by monitoring the fluorescence changes of **Mito-1**. HeLa cells were pretreated with DEA NONOate (NO donor) in the presence of sodium ascorbate, known to be a reducing agent, capable of converting NO to HNO.<sup>18</sup> The 3-dimensional co-localization image implied that **Mito-1** was predominantly localized in mitochondria over other organelles such as lysosome (Lyso) and endoplasmic reticulum (ER) (Fig. 4 and Fig. S18, ESI<sup>†</sup>). Altogether, these findings support our expectations on the ability of **Mito-1** to sense both exogenous HNO and endogenous HNO formation in mitochondria.

Finally, we evaluated the two-photon fluorescence properties of **Mito-1**, which allows us overcoming fluorescence interference from ubiquitous biological entities in cellular milieu.<sup>21</sup> As can be observed in Fig. 5, HNO (AS) pretreated HeLa cells were fluorescently labeled in the 420–520 nm range while excited at  $\lambda_{\text{ex}}$  740 nm in the presence of **Mito-1**. This result demonstrated that **Mito-1** has the ability to ensure mitochondrial endogenous

Fig. 3 Fluorescence and co-localization images under exogenous HNO sensing conditions. (A) Confocal microscopy co-localization images of **Mito-1** (5.0  $\mu\text{M}$ ) with organelle specific trackers (mitochondria, endoplasmic reticulum and lysosome). (B) Localization of the probe in mitochondria was confirmed by using Z-section images. (a) Z-section image of the cell, (b) co-localization with a mitochondria tracker and the probe, and (c) co-localization scatterplot (magnification,  $\times 63$ ).  $\lambda_{\text{ex}}$  405 nm;  $\lambda_{\text{em}}$  470–500 nm.

and exogenous HNO formation without any fluorogenic interference from inherent biological entities.

In conclusion, we demonstrated herein the synthesis and optical properties of a metal-free chemodosimetric turn-on fluorogenic probe **Mito-1**, for the sensing of nitroxyl (HNO) in mitochondria. The UV absorption at  $\lambda_{\text{abs}}$  398 nm and the fluorescence intensity at  $\lambda_{\text{em}}$  452 nm of **Mito-1** were  $\sim 25$  and  $\sim 45$ -fold enhanced in the presence of HNO (100  $\mu\text{M}$ ). The sensitivity of **Mito-1** toward nitroxyl was as low as 18 nM. The probe is also highly stable in a physiological pH range. It enables the visualization of mitochondrially localized endogenous and exogenous nitroxyl by providing a 'turn-on' fluorescence signal. The two-photon 'turn-on' fluorescence response in the presence of HNO in living cells allows overcoming interference from the omnipresent entities in living systems, making it a promising tool to detect mitochondrial nitroxyl.

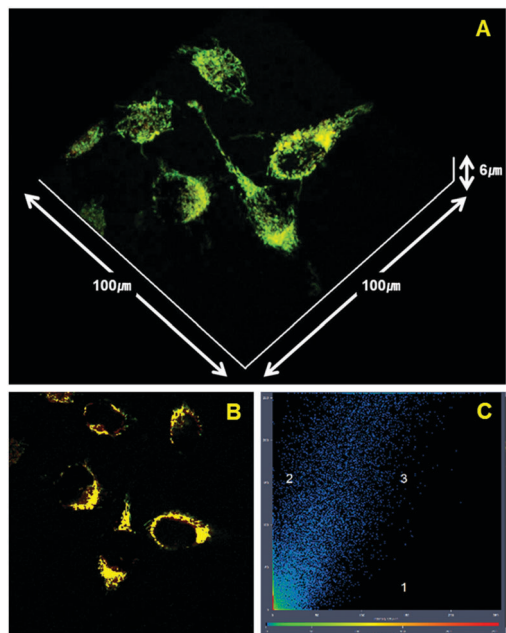


Fig. 4 Confocal microscopy co-localization images of endogenous HNO with probe and mitochondria organelle tracker. Co-localization of **Mito-1** (5.0  $\mu\text{M}$ ) for mitochondria was confirmed by using Z-section images of a confocal laser scanning microscope. (A) 3D image of the cell (B) co-localization with a mitochondria tracker and the probe (C) co-localization scatterplot.  $\lambda_{\text{ex}}$  405 nm;  $\lambda_{\text{em}}$  470–500 nm.

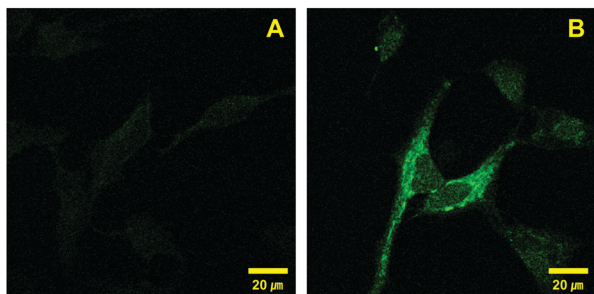


Fig. 5 Two photon fluorescence microscopy of **Mito-1** (10  $\mu\text{M}$ ) (A) in the absence of HNO and (B) in the presence of exogenous HNO.  $\lambda_{\text{ex}}$  740 nm;  $\lambda_{\text{em}}$  420–520 nm.

This work was supported by CRI (No. 2009-0081566, JSK) project grants and GPF grant (No. 2014H1A2A1020978, KS) from the National Research Foundation of Korea. SB thanks DST-SERB, India, for a research grant (No. ECR/2015/00035, SB).

## Notes and references

- 1 J. Hobbs, J. M. Fukuto and L. J. Ignarro, *Proc. Natl. Acad. Sci. U. S. A.*, 1994, **91**, 10992.
- 2 D. A. Wink, K. M. Miranda, T. Katori, D. Mancardi, D. D. Thomas, L. Ridnour, M. G. Espey, M. Feelisch, C. A. Colton, J. M. Fukuto, P. Pagliaro, D. A. Kass and N. Paolucci, *Am. J. Physiol.: Heart Circ. Physiol.*, 2003, **285**, H2264.
- 3 N. Paolucci, T. Katori, H. C. Champion, M. E. John, Et., K. M. Miranda, J. M. Fukuto, D. A. Wink and D. A. Kass, *Proc. Natl. Acad. Sci. U. S. A.*, 2003, **100**, 5537.
- 4 M. Shinyashiki, K. T. Chiang, C. H. Switzer, E. B. Gralla, J. S. Valentine, D. J. Thiele and J. M. Fukuto, *Proc. Natl. Acad. Sci. U. S. A.*, 2000, **97**, 2491.
- 5 H. T. Nagasawa, E. G. DeMaster, B. Redfern, F. N. Shiota and D. J. Goon, *J. Med. Chem.*, 1990, **33**, 3120.
- 6 O. Sidorkina, M. G. Espey, K. M. Miranda, D. A. Wink and J. Laval, *Free Radical Biol. Med.*, 2003, **35**, 1431.
- 7 W. K. Kim, Y. B. Choi, P. V. Rayudu, P. Das, W. Asaad, D. R. Arnelle, J. S. Stamler and S. A. Lipton, *Neuron*, 1999, **24**, 461.
- 8 M. G. Espey, K. M. Miranda, D. D. Thomas and D. A. Wink, *Free Radical Biol. Med.*, 2002, **33**, 827.
- 9 N. Paolucci, W. F. Saavedra, K. M. Miranda, C. Martignani, T. Isoda, J. M. Hare, M. G. Espey, J. M. Fukuto, M. Feelisch, D. A. Wink and D. A. Kass, *Proc. Natl. Acad. Sci. U. S. A.*, 2001, **98**, 10463.
- 10 (a) J. Rosenthal and S. J. Lippard, *J. Am. Chem. Soc.*, 2010, **132**, 5536; (b) M. Royzen, J. J. Wilson and S. J. Lippard, *J. Inorg. Biochem.*, 2013, **118**, 162; (c) Y. Zhou, K. Liu, Y. Y. Li, Y. Fang, T. C. Zhao and C. Yao, *Org. Lett.*, 2011, **13**, 1290; (d) A. T. Wrobel, T. C. Johnstone, A. D. Liang, S. J. Lippard and P. Livera-Fuentes, *J. Am. Chem. Soc.*, 2014, **136**, 4697.
- 11 M. R. Cline and J. P. Toscano, *J. Phys. Org. Chem.*, 2011, **24**, 993.
- 12 (a) K. Kawai, N. Ieda, K. Aizawa, T. Suzuki, N. Miyata and H. Nakagawa, *J. Am. Chem. Soc.*, 2013, **135**, 12690; (b) C. Liu, H. Wu, Z. Wang, C. Shao, B. Zhu and X. Zhang, *Chem. Commun.*, 2014, **50**, 6013; (c) G. J. Mao, X. B. Zhang, X. L. Shi, H. W. Liu, Y. X. Liu, H. Y. Zhou, W. Tan and R. Q. Yu, *Chem. Commun.*, 2014, **50**, 5790; (d) Z. Miao, J. A. Reisz, S. M. Mitroka, J. Pan, M. Xian and S. B. King, *Bioorg. Med. Chem. Lett.*, 2015, **25**, 16; (e) K. Zheng, W. Lin, D. Cheng, H. Chen, Y. Liu and K. Liu, *Chem. Commun.*, 2015, **51**, 5754; (f) K. N. Bobba, Y. Zhou, L. E. Guo, T. N. Zang, J. F. Zhang and S. Bhuniya, *RSC Adv.*, 2015, **5**, 84543; (g) X. Zhu, M. Xiong, H.-W. Liu, G.-J. Mao, L. Zhou, J. Zhang, X.-B. Zhang and W. Tan, *Chem. Commun.*, 2016, **52**, 733.
- 13 (a) M. H. Lee, S. W. Lee, S. H. Kim, C. Kang and J. S. Kim, *Org. Lett.*, 2009, **11**, 2101; (b) H. S. Jung, J. H. Han, Y. Habata, C. Kang and J. S. Kim, *Chem. Commun.*, 2011, **47**, 5142; (c) H. S. Jung, J. H. Han, Z. H. Kim, C. Kang and J. S. Kim, *Org. Lett.*, 2011, **13**, 5056.
- 14 (a) X. Jing, F. Yu and L. Chu, *Chem. Commun.*, 2014, **50**, 14253; (b) Y. Tan, R. Liu, H. Zhang, R. Peltier, Y.-W. Lam, Q. Zhu, Y. Hu and H. Sun, *Sci. Rep.*, 2015, **5**, 16979.
- 15 (a) H. De Vitto, B. S. Mendonça, K. M. Elseth, A. Onul, J. Xue, B. J. Vesper, C. V. Gallo, F. D. Rumjanek, W. A. Paradise and J. A. Radosevich, *Tumour Biol.*, 2013, **34**, 403; (b) A. Augustyniak, J. Skolimowski and A. Blaszczyk, *Chem.-Biol. Interact.*, 2013, **206**, 262.
- 16 S. Shiva, J. H. Crawford, A. Ramachandran, E. K. Ceaser, T. Hilldon, P. S. Brookes, R. P. Patel and V. M. Darley-Usmar, *Biochem. J.*, 2004, **379**, 359.
- 17 X. Gong, X.-F. Yang, Y. Zhong, Y. Chen and Z. Li, *Dyes Pigm.*, 2016, **131**, 24.
- 18 S. Maiti, N. Park, J. H. Han, H. M. Jeon, J. H. Lee, S. Bhuniya, C. Kang and J. S. Kim, *J. Am. Chem. Soc.*, 2013, **135**, 4567.
- 19 M. H. Lee, N. Park, C. Yi, J. H. Han, J. Hong, K. P. Kim, D. H. Kang, J. L. Sessler, C. Kang and J. S. Kim, *J. Am. Chem. Soc.*, 2014, **136**, 14136.
- 20 (a) W. S. Shin, M. G. Lee, P. Verwilst, J. H. Lee, S. G. Chi and J. S. Kim, *Chem. Sci.*, 2016, **7**, 6050; (b) H. S. Jung, J. Han, J.-H. Lee, J. H. Lee, J.-M. Choi, H.-S. Kweon, J. H. Han, J. H. Kim, K. M. Byun, J. H. Jung, C. Kang and J. S. Kim, *J. Am. Chem. Soc.*, 2015, **137**, 3017.
- 21 (a) Y. H. Lee, W. X. Ren, J. Han, K. Sunwoo, J.-Y. Lim, J.-H. Kim and J. S. Kim, *Chem. Commun.*, 2015, **51**, 14401; (b) J. F. Zhang, C. S. Lim, S. Bhuniya, B. R. Cho and J. S. Kim, *Org. Lett.*, 2011, **13**, 1190.